Available online at www.sciencedirect.com
ScienceDirect
Cryobiology 55 (2007) 200–209
CRYOBIOLOGY
www.elsevier.com/locate/ycryo

Development of a microfluidic device for determination of cell osmotic behavior and membrane transport properties ☆

Hsiu-hung Chen [a], Jester J.P. Purtteman [a], Shelly Heimfeld [c], Albert Folch [a,b,*], Dayong Gao [a,d,*]

[a] Department of Mechanical Engineering, University of Washington, ME Building R254, Seattle, WA 98195, USA
[b] Department of Bioengineering, University of Washington, William H. Foege Building, Rm. N430-N, 1705 NE Pacific St., Campus Box 355061, Seattle, WA 98195, USA
[c] Bone Marrow Transplant Program, Fred Hutchinson Cancer Research Center, Seattle, WA, USA
[d] Department of Mechanical Engineering and Center for Biomedical Engineering, University of Kentucky, Lexington, KY, USA

Received 9 August 2006; accepted 6 August 2007
Available online 24 August 2007

Abstract

An understanding of cell osmotic behavior and membrane transport properties is indispensable for cryobiology research and development of cell-type-specific, optimal cryopreservation conditions. A microfluidic perfusion system is developed here to measure the kinetic changes of cell volume under various extracellular conditions, in order to determine cell osmotic behavior and membrane transport properties. The system is fabricated using soft lithography and is comprised of microfluidic channels and a perfusion chamber for trapping cells. During experiments, rat basophilic leukemia (RBL-1 line) cells were injected into the inlet of the device, allowed to flow downstream, and were trapped within a perfusion chamber. The fluid continues to flow to the outlet due to suction produced by a Hamilton Syringe. Two sets of experiments have been performed: the cells were perfused by (1) hypertonic solutions with different concentrations of non-permeating solutes and (2) solutions containing a permeating cryoprotective agent (CPA), dimethylsulfoxide (Me_2SO), plus non-permeating solute (sodium chloride (NaCl)), respectively. From experiment (1), cell osmotically inactive volume (V_b) and the permeability coefficient of water (L_p) for RBL cells are determined to be 41% [$n = 18$, correlation coefficient (r^2) of 0.903] of original/isotonic volume, and 0.32 ± 0.05 μm/min/atm ($n = 8$, $r^2 > 0.963$), respectively, for room temperature (22 °C). From experiment (2), the permeability coefficient of water (L_p) and of Me_2SO (P_s) for RBL cells are 0.38 ± 0.09 μm/min/atm and $(0.49 \pm 0.13) \times 10^{-3}$ cm/min ($n = 5$, $r^2 > 0.86$), respectively. We conclude that this device enables us to: (1) readily monitor the changes of extracellular conditions by perfusing single or a group of cells with prepared media; (2) confine cells (or a cell) within a monolayer chamber, which prevents imaging ambiguity, such as cells overlapping or moving out of the focus plane; (3) study individual cell osmotic response and determine cell membrane transport properties; and (4) reduce labor requirements for its disposability and ensure low manufacturing costs.

Keywords: Microfluidic; Perfusion system; RBL-1; Permeability coefficient of water; Permeability coefficient of Me_2SO; Monolayer; Soft lithography

During cooling, warming, addition or removal of cryopreservative agents (CPAs), cells experience a series of highly anisotonic conditions, which can cause injury to cells [23]. The transport of water across the cell membrane and intracellular water content play critical roles in cell viability and lethal intracellular ice formation (IIF) during cooling and warming [22–24,28,31,36]. During CPA addition before freezing and removal after thawing, cells may undergo detrimental osmotic volume changes if unsuitable processes are applied [5,9,34]. In order to prevent cryoinjury, as well as optimize cryopreservation protocols, several important cell

☆ This work was supported by a grant from NIH FHCRC/UW Center for Medical Countermeasures against Radiation and a Gift grant from Washington Research Foundation.
* Corresponding authors. Fax: +1 206 685 8047 (D. Gao).
E-mail addresses: afolch@u.washington.edu (A. Folch), dayong@u.washington.edu (D. Gao).

0011-2240/$ - see front matter © 2007 Elsevier Inc. All rights reserved.
doi:10.1016/j.cryobiol.2007.08.001

membrane transport properties have to be determined. These biophysical properties are: (1) the cell membrane permeability coefficient of water (L_p); (2) the cell membrane permeability coefficient of cryoprotective agents (P_s) (CPAs); (3) reflection coefficients (σ) of the cell membrane to CPAs; and (4) the activation energies of these permeability coefficients. Knowing these permeability properties will make it possible to develop optimal protocols for the addition and removal of cryoprotectant, and optimal cooling or thawing rates for cells [2,9,12,23,27,31,36].

Various devices, which are extensively reviewed by McGrath [30], have been developed to quantify the cell membrane transport properties that are mentioned in the preceding paragraph by means of nuclear magnetic resonance [33], "stop flow" [21], electron paramagnetic resonance [16], electronic sizing [11,19,26], and light microscopy [8,10,18,29]. Of these methods, light microscopy is the only one that has been used to determine membrane transport properties of either a large cell population or a single cell. This technique can be used to directly observe, trace, and analyze the volume changes of single cells in anisotonic environments. A microdiffusion system developed by McGrath [29] has been proved to be very effective in determining the water permeability of several types of cell lines by using light microscopy. This system comprises a main channel for the bulk flow of desired solutions, a chamber which serves as a sample region, and a dialysis membrane, between the chamber and the channel, to immobilize the cells. Two potential problems may occur while using this system: (a) ripping the dialysis membrane unintentionally when the microdiffusion chamber is formed and (b) the introduction of additional mathematical complexity due to the presence of the dialysis membrane [29,30]. Gao et al. [10] developed a microperfusion technique to determine the membrane transport properties of mouse oocytes. In their experiment, individual mouse oocytes are hold using a micropipette by applying a small negative pressure to the zona pellucida. The immobilized mouse oocyte is then directly perfused by another micropipette with an anisotonic solution. Using this technique, water, dimethylsulfoxide (Me_2SO), and propylene glycol (PG) permeability coefficients of the mouse oocytes were determined. Although the microperfusion technique simplifies the mathematical formulation and overcomes the problems related with the microdiffusion technique, a glass micropipette can only be used with cell types having "shells" (e.g. zona pellucida for oocytes). Moreover, each glass micropipette can hold only one cell during the course of the perfusion and measurement, further restricting this technique to small numbers of cells. Combining elements of the microdiffusion chamber and the micropipette perfusion method, Gao et al. [8] later presented a microperfusion chamber capable of manipulating multiple, or single, cells and different cell types (e.g. mouse oocytes and golden hamster pancreatic islet cells). Rather than being held by the micropipette, cells are immobilized on a transparent porous membrane (average pore size: 1–2 μm), at the bottom of the cavity and are then perfused instantaneously by the second solution, whose flow rate is controlled by a Hamilton Syringe. The chamber cavity and porous membrane overcome the single cell limitation of micropipette perfusion and avoid the mathematical complexity of the microdiffusion method. However, in order to assure the effectiveness of this device, the membrane pores have to be large enough and/or numerous enough to produce a fast environment change, and also small enough to prevent cells of interest from squeezing out. That means customized porous membranes may be needed to immobilize different cell types and still provide the ability to instantaneously replace the medium. On the other hand, washing the chamber after use and reassembling all parts together for each use makes this process labor intensive. Takamatsu et al. [37] developed a perfusion microscope to study the osmotic response of human prostatic adenocarcinoma cells (PC-3) that attached on a glass surface or a thin mesh cloth to immobilize cells. However, this approach is limited to adherent cells.

Microfluidic systems fabricated in poly(dimethylsiloxane) (PDMS) using soft lithography techniques have many advantages over conventional systems [1,7,25,32,35,38–40] and have been employed in the study of the osmotic behavior of cells for years [3,4,13]. To the best of our knowledge, no determination of membrane transport properties for a single cell has been previously demonstrated on PDMS-based microfluidic devices. In the present study, we have developed a microfluidic perfusion system with disposable parts that does not suffer from the limitations and inconveniences stated in the preceding paragraph. The developed microfluidic perfusion chamber allows for passively trapping cells in a monolayer. The system is comprised of an inlet, microfluidic channels, a perfusion chamber, and an outlet and is made in PDMS. In our design, different heights (analogous to different sizes of pores for porous membranes) of microfeatures can be manufactured using a single mask. The master with desired microfeatures on it permits users to replica-mold each additional device in a couple of hours many times without showing any noticeable defects on the masters. The benefits of this system are: (1) disposability, reducing labor requirements, including washing and reassembling chamber parts, for multiple usages and (2) customizing the needed size and geometry of the chamber with just a change of the mask. In the following sections, we describe the experimental details and discuss several possible modifications and potential applications.

Materials and methods

Source of cells

Rat basophilic leukemia cells (RBL-1 line) were purchased from ATCC (American Type Culture Collection, Manassas, VA) and kindly donated by the Folch Lab (Department of Bioengineering, University of Washing-

ton). These cells were cultured using Dulbecco's Modified Eagle's Medium (DMEM, Life Technologies) with 10% fetal bovine serum (FBS, HyClone Inc., Logan UT) along with 100 U/mL penicillin (antibiotic–antimycotic, Life Technologies) and 100 μg/mL streptomycin, and were maintained in T25 flasks (Corning) inside an incubator at 37 °C in a humidified atmosphere containing 5% CO_2. RBL-1 is a suspension cell line, so the cells have a highly spherical shape, which is convenient for analyzing the cells using light microscopy and makes this cell line a good testing model for development of the microfluidic device and studies of cell membrane transport properties.

Preparation of cell suspensions

On the day of the experiment, RBL cells, diameter in the range of 15–20 μm, were collected, centrifuged, and resuspended in 1× phosphate buffered saline (PBS) (300 mOsm) at a cell density of about 5×10^4/mL, counted by a hemacytomer, and used within 3 h.

Design and fabrication for microfluidic perfusion chamber

Our design immobilizes single cells while preventing them from piling up on each other by restricting the volume available above them, as shown schematically in Fig. 1. The area encompassed by dotted lines represents the microfluidic perfusion chamber: cells flow from inlet (left in this diagram) to outlet (right) and are trapped here by a block, while the fluid keeps flowing through the bottom of the microchannel. The height of microchannel from inlet (h_2) confines the movement of cells. To allow cells to flow freely from inlet to the chamber, h_2 should be larger than the diameter of cells (Φ) but less than $2 \times \Phi$ (to maintain a monolayer of cells in the channel). The height of the slit (h_1), between the bottom of the channel and the block, should be smaller than Φ. We have found that it is best to make $h_1 < \Phi/2$ in order to prevent cells from squeezing into the slot. Since the diameter of the RBL cells (Φ) ranges from 15 μm to 20 μm, the dimensions for h_1 and h_2 were chosen to be 5 μm and 25 μm, respectively, and the channel width was chosen to be 150 μm wide.

Fabrication of the device, shown in Fig 1, in PDMS (Sylgard 184, Dow-Corning) was done by soft-lithographic rapid prototyping and replica molding. Fig. 2 depicts the schematic procedures for manufacturing of microfluidic devices in PDMS. From Fig. 2a–f, rapid prototyping was utilized in making a master containing the necessary microfluidic structures. Layouts of the design were created as a computer-aided design (CAD) file using AutoCAD (Autodesk Inc., San Rafael, CA). The CAD file was then sent to be printed onto a 2000 dpi, high-resolution transparency (CAD/Art Service Inc., Bandon, OR), which serves as a photomask. In order to construct 2-level features, 2 different layers of photoresist (SU8, MicroChem) were spin coated. The first layer, spun with SU8-5 at 500 rpm for 10 s and 2950 rpm for additional 30 s, on a silicon wafer was softbaked (to evaporate the solvent and to densify the film) and was then exposed to UV light (to polymerize the exposed region) through the photomask for 60 s (Fig. 2a). After softbaked and developed (Fig. 2b and c), the structure was left on the wafer. The second layer, spun on top of the first with

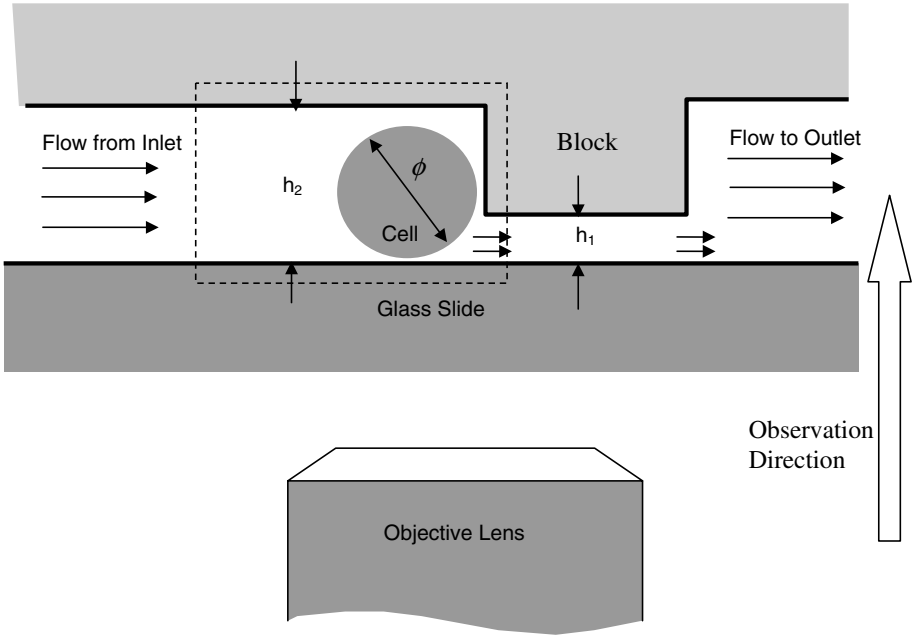

Fig. 1. Schematic diagram showing cell trapped in microfluidic perfusion chamber and monitored through microscope. h_1 is the height of the slit and h_2 is the height of the main microchannel. The solutions are allowed to flow through the slit. Cells, whose diameters are larger than the height of the slit, may hardly pass the slit.

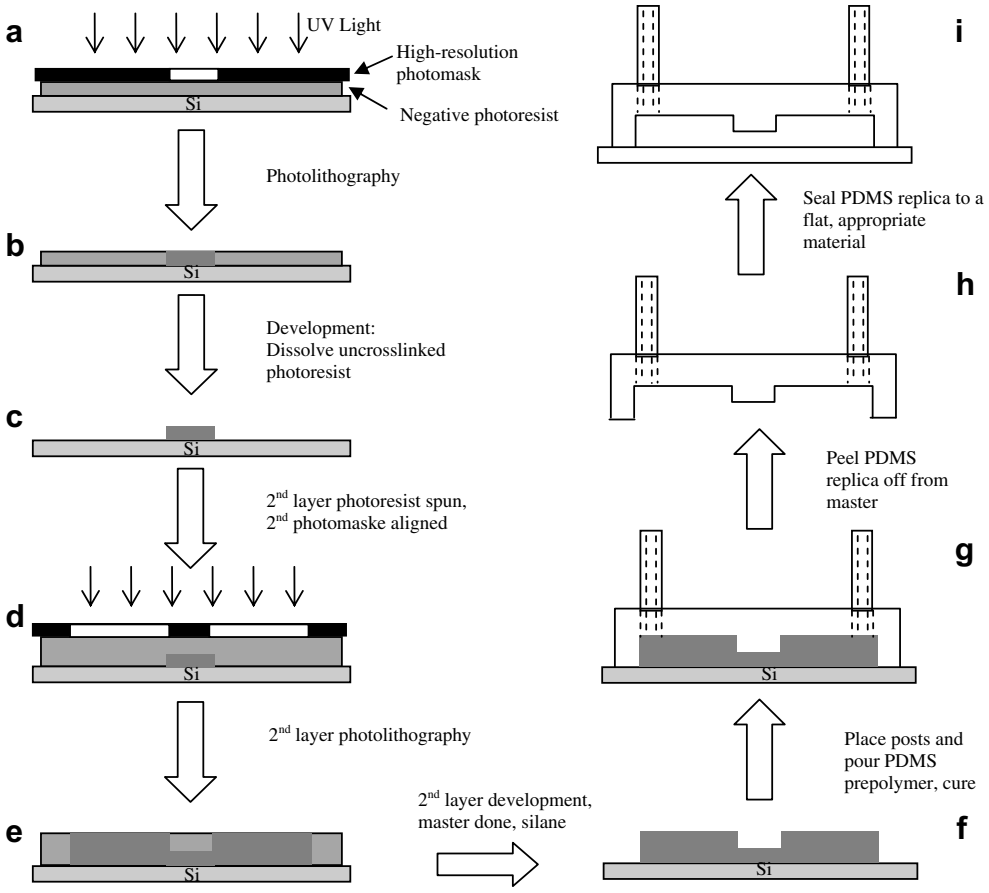

Fig. 2. Fabrication procedures of 2-layer microfluidic PDMS device utilizing rapid prototyping and replica molding.

SU8-25 at 500 rpm for 10 s and 2000 rpm for additional 30 s, was softbaked, UV exposed for 110 s through a different photomask, and then developed, as shown in Fig. 2d–f. Height measurement of structures using Surface Profilometer (Alpha Step 200, Tencor) indicates 3.8 μm and 22.7 μm for h_1 and h_2, respectively. The master was exposed to the vapor of tridecafluouro-1,1,2,2-tetrahydrooctyl-1-trichlorsilane (UCT Inc.) for ~30 min to prevent bonding between the master surface and the PDMS. Two possible ways can be applied for fluidic ports of the device: (1) two silicone tubes (ID = 1.59 mm, OD = 3.18 mm) which served as inlet and outlet, were glued on the expected positions before a mixture of PDMS prepolymer and curing agent, 10:1 in weight, was poured over the master (Fig. 2g), or (2) repeat (1) except gluing one silicone tube on the outlet position only, then cut a cubical hole (around 4 mm × 4 mm × 2 mm) by hand using a scalpel for inlet directly after the PDMS had been cured and placed on a glass slide. After curing in the oven at 65 °C for 2 h, a negative relief made in PDMS of the structure on the master was peeled off (Fig. 2h). To ensure a tight seal, both surfaces of PDMS device and the substrate (glass slide in this experiment) were exposed to oxygen plasma [25] at 150 W for 15 s. Finally, the PDMS device was irreversibly sealed on a glass slide, as shown in Fig. 2i. Fig. 3 shows the photo of this PDMS microfluidic perfusion device. Shown in Fig. 4a is a top-down view of the microfluidic perfusion chamber; the perfusion chamber is highlighted with dashed lines. Black lines, with arrows through the channel and the chamber, represent the nominal flow field. Five cells were clearly trapped within the microfluidic perfusion chamber (Fig. 4b).

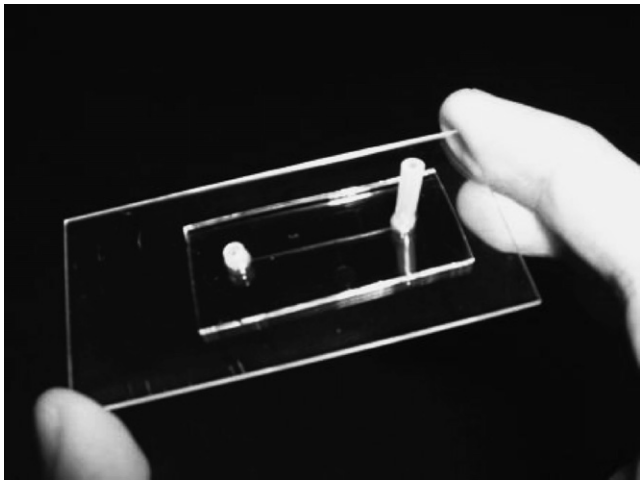

Fig. 3. PDMS microfluidic perfusion device irreversibly sealed on a glass slide.

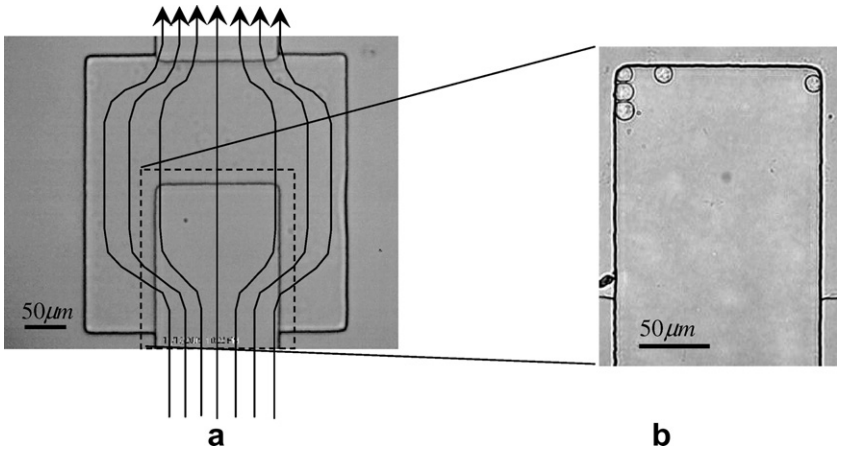

Fig. 4. Top-down view of microfluidic perfusion chamber (a) direction of the flow shown in arrows (b) RBL-1 cells were constrained within the chamber.

Validation of replacement time between different media

Although instantaneous step change of extracellular concentration has been claimed/assumed in previous devices [8,10,30], this transient procedure, until it reaches the steady state, requires time (replacement time). In order to validate how long it takes for the succeeding medium to substitute from the original one in our device, 1× PBS was first added to the channel, followed by perfusion with a fluorescein (Acid Yellow 73, Sigma–Aldrich). Fluorescent images within the microperfusion chamber were acquired with a fluorescent microscope system, comprising a CCD camera (ORCA-HR, Hamamatsu Photonics, Hamamatsu City, Japan) and an inverted microscope (TE2000-U, Nikon). The replacement time between two media could be determined by measuring the concentration increase of the fluorescein at the location of interest in the channel.

System setup and manipulation procedures

The experimental setup of the microfluidic perfusion system is shown in Fig. 5. The microfluidic perfusion chamber device, made in PDMS and irreversibly sealed on a glass slide, is mounted on the stage of an inverted microscope (TE2000-S, Nikon). In order to perform continuous aspiration, a Hamilton Syringe is connected through a silicone tube to the outlet of the device. In experiments, 1× PBS is first injected into the inlet to rinse the channel. Due to the oxygen plasma treatment, the surfaces of glass and PDMS inside the channel are highly hydrophilic, and medium fills the channel quickly. Bubbles may form inside the chamber, but quickly disappeared. The cell suspension is later injected into the same inlet. With continual sucking by the Hamilton Syringe, cells flow through the channel and are trapped in the perfusion chamber. At the same time, part of the cell suspension solution continues moving downstream through the bottom slit. Once the number of cells is enough for the experiment (usually 10–15), the original cell suspension solution is replaced by the new PBS solution with different concentrations of electrolytes (1.5×, 2×, and 3×), or 1.5 M Me_2SO solution which is isotonic with respect to NaCl (0.9% NaCl). The new medium should be injected in less than half a second in large enough amount (0.5 mL) until the silicone tubing ($D = 1.58$ mm × 4 mm) or the cubical hole (4 mm × 4 mm × 2 mm) is filled so that residual cell suspension (~1 μL) would not affect the desired concentration. Before, during, and after the perfusion process, the cell volume changes are recorded by a CCD camera (Fusion, Logitech Inc., Fremont, CA), which is connected to the computer, until osmotic equilibrium between the intracellular and extracellular environments is achieved.

Evaluation of water permeability coefficient

The water permeability coefficient (L_p), and osmotically inactive volume (V_b) of RBL-1 cells were determined by measuring changes in cell volume while cells were perfused (in the microfluidic perfusion system) by anisotonic PBS solutions, where only a non-permeating solute was present, using light microscopy. Cell volume was measured from captured cell images by counting the number of pixels of each cell in Matlab (The Mathworks, Inc., Natick, MA). The data were then fitted to the following differential equation to determine L_p, using MLAB (Civilized Software Inc., Silver Spring, MD), which describes the rate of water movement across the cell membrane [6,27]:

$$\frac{dV_c(t)}{dt} = L_p \cdot A \cdot (C_n^i - C_n^e) \cdot R \cdot T \quad (1)$$

where $V_c(t)$ = cell volume (μm^3), t = time (s), L_p = water permeability coefficient of cell membrane (μm/min/atm), A = cell surface area (assumed to be constant, μm^2), C_n^i=intracellular osmolality (Osm/kg(water)), C_n^e=extracellular osmolality (Osm/kg(water)), R = universal gas constant [0.08207 atm L/(mole K)], and T = absolute temperature (K). The intracellular osmolality during hypertonic shrinkage can be determined using the Boyle van't-

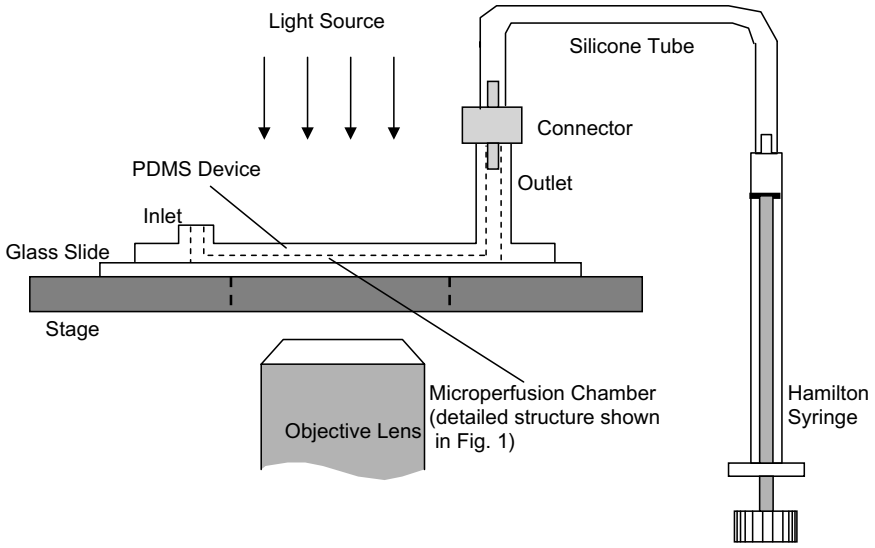

Fig. 5. Experimental setup of the microfluidic perfusion system. Cell suspension and prepared medium with different concentrations were injected in inlet while fluid was aspirated continually from outlet using Hamilton Syringe. Cell volume response was observed using an inverted microscope throughout the experiment.

Hoff relationship applied to the osmotic responses of cells [20]:

$$C_n^{\mathrm{i}} = C_0 \cdot \left(\frac{V_0 - V_{\mathrm{b}}}{V - V_{\mathrm{b}}}\right) \tag{2}$$

where C_0 = isotonic osmolality (Osm/kg(water)), V_0 = isotonic cell volume (μm^3), and V_{b} = osmotically inactive cell volume (μm^3). For RBL-1 cells, the V_{b} value was determined by a Boyle van't-Hoff plot [18,20] after cells were perfused and osmotically equilibrated with various PBS solutions with different salt concentrations (1.5×, 2×, and 3× isotonic concentration). The L_{p} value of cells at room temperature (22 °C) was determined by least-square curve fitting [9,10,18,20,29,30] after cells were perfused by 2× and 3× PBS solutions.

Determination of CPA permeability of cell membrane: two-parameter transport formalism

When both permeable solute (e.g. permeating CPA) and non-permeating solute (e.g. salts) are present in a solution, the two-parameter transport formalism can be used to determine the water permeability, L_{p}, and solute permeability, P_{s} [15,17].

Compared with Eq. (1), the cell volume change is governed not only by non-permeating solute, but also by the concentration of permeating solutes,

$$\frac{\mathrm{d}V_{\mathrm{c}}(t)}{\mathrm{d}t} = \frac{\mathrm{d}V_{\mathrm{s}}(t)}{\mathrm{d}t} + L_{\mathrm{p}} \cdot A \cdot (C^{\mathrm{i}} - C^{\mathrm{e}}) \cdot R \cdot T \tag{3}$$

and the solute flux is given by

$$\frac{\mathrm{d}N_{\mathrm{s}}(t)}{\mathrm{d}t} = P_{\mathrm{s}} A (C_{\mathrm{s}}^{\mathrm{e}} - C_{\mathrm{s}}^{\mathrm{i}}), \tag{4}$$

where C^{i} and C^{e} are total intracellular and extracellular osmolality (Osm/kg(water)), respectively, $C_{\mathrm{s}}^{\mathrm{i}}$ and $C_{\mathrm{e}}^{\mathrm{s}}$ are intracellular and extracellular osmolality of permeating solutes (Osm/kg(water)), respectively, $V_{\mathrm{s}}(t)$ is intracellular volume of permeating solute (μm^3), N_{s}(t) is the number of osmoles of permeating solute in the cell and P_{s} is the solute permeability (cm/min). $N_{\mathrm{s}}(t)$ and $V_{\mathrm{s}}(t)$ are interchangeable for

$$N_{\mathrm{s}}(t) = V_{\mathrm{s}}(t)/\overline{V}_{\mathrm{s}} \tag{5}$$

where $\overline{V}_{\mathrm{s}}$ is partial molar volume of permeating solute (μm^3). The L_{p} and P_{s} values of cells at room temperature (22 °C) were determined by least-square curve fitting [9,10,18,20,29,30] after cells were perfused by 1.5 M Me_2SO solution isotonic with respect to NaCl.

Results

Replacement time of solution in microfluidic channel

As indicated in the Materials and methods, for the experiment to evaluate the replacement time between 2 media, 1× PBS was first perfused through the channel, followed by a medium with fluorescein. Fig. 6a, the fluorescent image acquired with a fluorescent microscopy system, shows the top-down view of the channels and the chamber (position of the walls indicated by the dashed lines), and a solid line, in which the monitoring position is located. The position is chosen because this is where most of the cells would be immobilized. Fig. 6b represents the relative concentrations, which were areas under different concentration profiles at every 0.1 s, with the average flow speed of about 1150 μm/s (or 5 nL/s) along a 5 mm-long channel, measured from the inlet to the chamber. The relative fluorescein concentration at 0.2 s and 0.9 s reached 10% and 90%, respectively, if the original fluores-

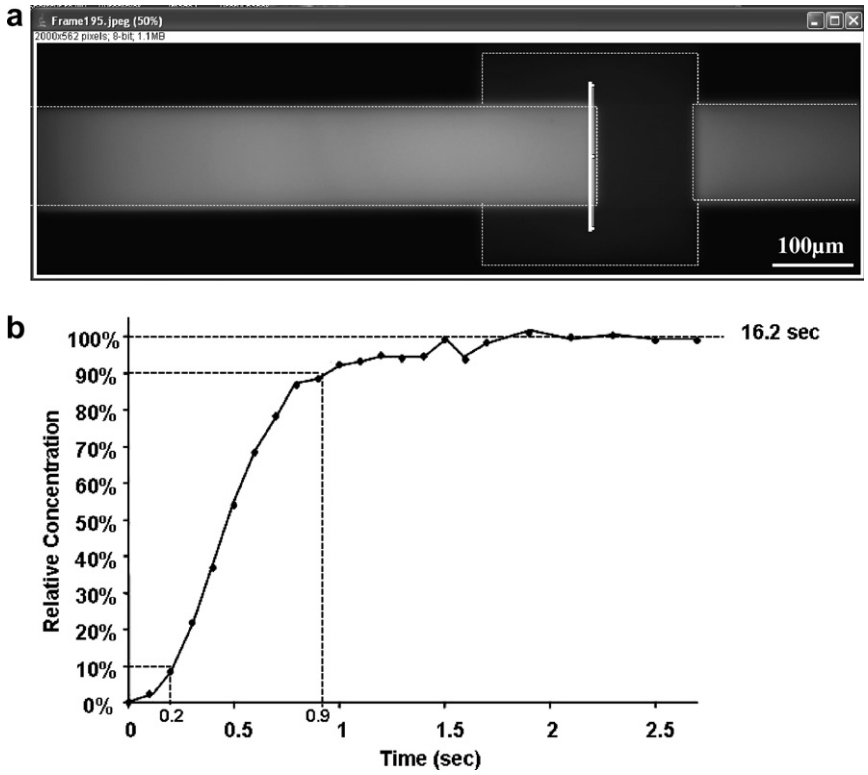

Fig. 6. Measurement of the time needed to replace one solution (water) with another (fluorescein). (a) Top-down view of the channel and perfusion chamber (walls marked by dashed lines), and the monitoring position (marked by solid line) and (b) relative concentration history at monitoring position.

cein concentration is treated as 100%. Time for replacement is around 1.7 s or shorter from 0% to near 100% when the flow speed is controlled at 400 μm/s (or 1.8 nL/s) or faster, since the Reynolds number is low ($Re \sim 0.025$) and diffusion at the boundary between two consecutive solutions is negligible.

Determination of L_p and V_b

Two Boyle van't Hoff plots are shown in Fig. 7a and b. The inactive volume V_b of RBL cells, which was determined to be 41% [$n = 18$, correlation coefficient (r^2) of 0.903] of original/isotonic volume by the perfusion method, is comparable to the value of 39% ($n = 40$, $r^2 = 0.986$) of original/isotonic volume obtained by the diffusion method [18,20].

Fig. 8 shows photographs of RBL cells perfused with hypertonic 3× PBS. The big arrow depicts the direction of the flow. Cells were trapped within the perfusion chamber while the medium flowed downstream by suction, as shown in Fig. 8a. A magnified view, Fig. 8b, shows two intact cells which were right before exposure to the hypertonic solution, or at $t = 0$. The photographs of the cell volume changes after they were exposed to the hypertonic solution at 10 s, 20 s,

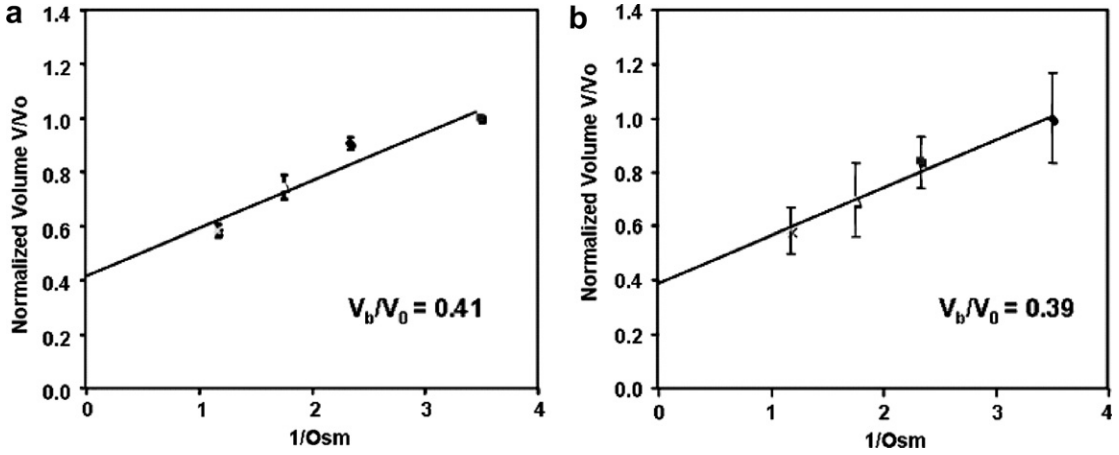

Fig. 7. Boyle Van't-Hoff relationship for RBL cells at room temperature (22 °C), (a) by perfusion method, mean ± SD ($n = 18$, $r^2 = 0.903$) and (b) by diffusion method, mean ± SD ($n = 40$, $r^2 = 0.986$). Cells are randomly collected for measurements in (b). Inactive cell volume V_b were determined to be 0.41 and 0.39 of original/isotonic volume for perfusion method and diffusion method, respectively.

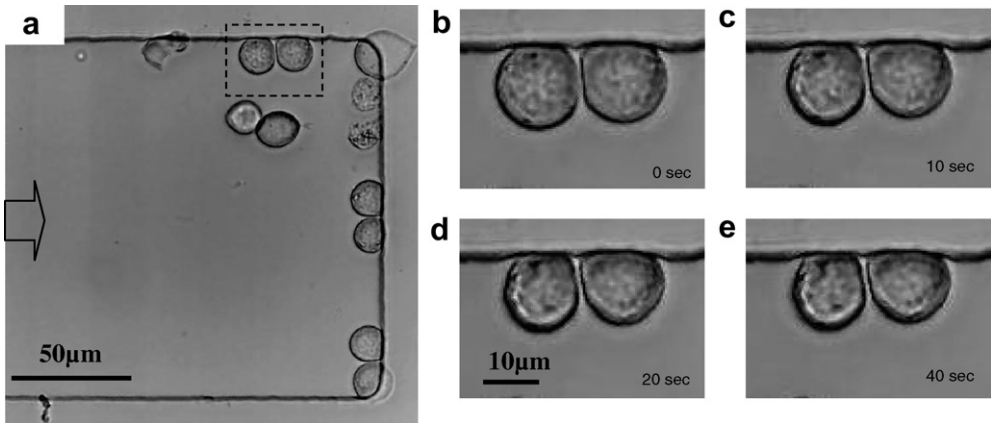

Fig. 8. (a) RBL Cells trapped within the perfusion chamber and (b) a magnified view inside dashed line when cells were perfused by 2× hypertonic PBS at times $t = 0$ s, (c) $t = 10$ s, (d) $t = 20$ s, and (e) $t = 40$ s.

and 40 s, are shown in Fig. 8c, d, and e, respectively. Cells kept shrinking, from Fig. 8b–e, until they reached the osmotic balance between intracellular and extracellular solutions. The history of volume change of RBL cells was then processed using Matlab, and water permeability coefficient L_p was determined by curve fitting (using Eqs. (1) and (2)) to be 0.32 ± 0.05 μm/min/atm ($n = 8$, $r^2 > 0.963$) at 22 °C using MLAB, as shown in Fig. 9. These data are similar to those reported for other cell types in references, observed by using light microscopy (Table 1).

Fig. 10 shows the cell volume change after being perfused by 1.5M Me_2SO solution isotonic with respect to NaCl. Water permeability coefficient L_p and Me_2SO permeability P_s of the cells were determined by curve fitting (using Eqs. (3)–(5)) to be 0.38 ± 0.09 μm/min/atm and $(0.49 \pm 0.13) \times 10^{-3}$ cm/min ($n = 5$, $r^2 > 0.86$) at 22 °C, respectively.

Discussion and conclusion

A microfluidic perfusion device is developed in this study to determine the osmotic behavior and transport properties of cell membranes using rat basophilic leukemia cells (RBL-1 line) as a cell model. A perfusion flow speed >400 μm/s (or 1.8 nL/s) along the main microchannel will ensure less than 1.7 s replacement time of a new solution in the microfluidic device. This solution replacement time can be further reduced if the perfusion flow speed is increased. It should be mentioned that in the mathematical modeling and curve fitting, we assumed a 0 s replacement time (i.e. the extracellular environment was replaced by

Table 1
A comparison of water permeability for mammalian cells determined using light microscopy method

Cell type	L_p (μm/min/atm)	Reference
Rat basophilic leukemia	0.32 ± 0.05 (22 °C)	Present
Mouse ovum	0.43 (20 °C)	[18]
Mouse oocyte	0.48 ± 0.2 (20 °C)	[14]
Mouse oocyte	0.45 ± 0.11 (22 °C)	[10]
Golden hamster pancreatic islet	0.27 ± 0.08 (22 °C)	[8]
Human prostate cancer cell	0.45 (23 °C)	[37]

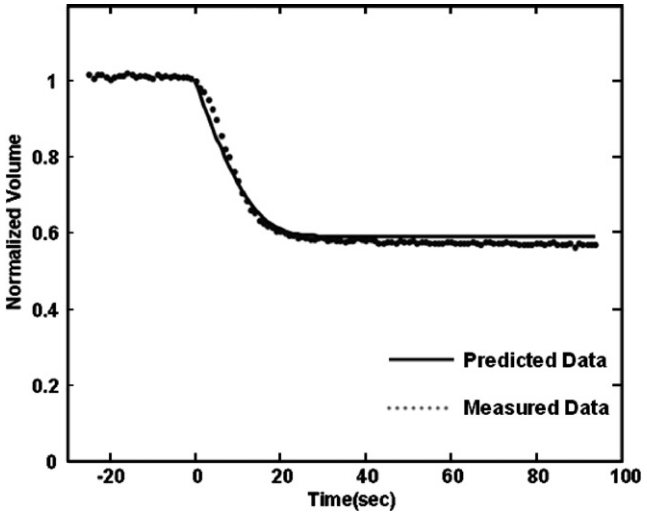

Fig. 9. Volume change of RBL cells in response to 3× PBS, $r^2 = 0.973$.

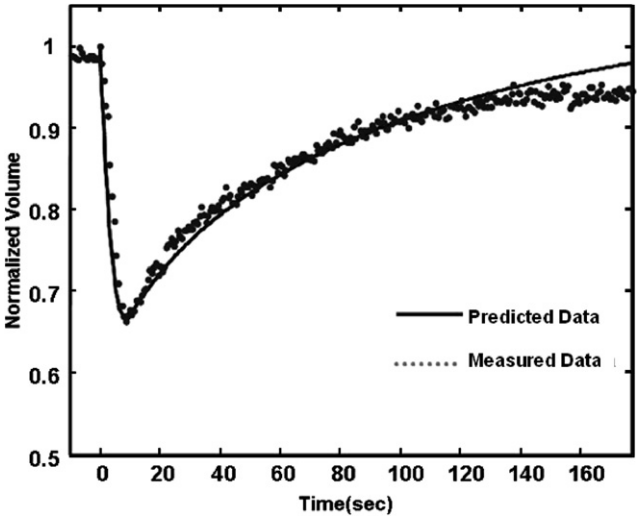

Fig. 10. Volume change of RBL cells in response to 1.5 M Me_2SO plus 0.9% NaCl, $r^2 = 0.947$.

the perfusion solution instantaneously) which induces a certain degree of inconsistency and error between the real experimental condition and theoretical assumption. Hinted by the measured data of relative concentration shown in Fig. 6b, one possible way to compensate a non-zero replacement time is to simply replace the constant extracellular osmolality (C^e) with a time-variant function,

$$C^e(t) = A \times (1 - e^{-Bt}) \quad (6)$$

where A is ultimate osmolality (Osm/kg(water)), and B is time constant (1/s). A and B will be 0.9 and 1.354, respectively, if cells are perfused with 3× PBS at 400 μm/s (or 1.8 nL/s) and the extracellular environment reaches 90% of its ultimate osmolality. A curve-fitted line (dashed, using Eqs. (1), (2), and (6)) is shown in Fig. 11, and is compared with the measured data and the curve-fitted data without compensation. A 0.03 μm/min/atm (or 8%) increase of L_p is obtained from the compensated curve-fitting. Experimental results have also shown that the shape of some cells tend to become irregular during dehydration. This can also introduce errors in analysis since the fundamental assumption of the light microscopy method is based on spherical cellular shapes. A 3D image reconstruction through different focusing planes during perfusion can be one of possible treatments towards the uncertainty of the cell volume measurement.

In summary, the microfluidic perfusion chamber made in PDMS using soft lithography has proved to be useful for confining cells within a perfusion chamber. PDMS is transparent, so it allows for light microscopy monitoring of cell volume changes. By analyzing captured images of cell volume changes during perfusion, inactive cell volume V_b, water permeability coefficient L_p, and Me_2SO permeability coefficient P_s can be determined. The present study is focused on testing the concept, which has been successfully proved, of device production and cell osmotic responses by the use of RBL cell line as a model. As we know, the osmotic behavior and permeability of cells are temperature dependent. A temperature control device has been developed and will be used to control the temperature in the microfluidic perfusion system to study cell permeability at various temperatures, ranging from 37 to −15 °C.

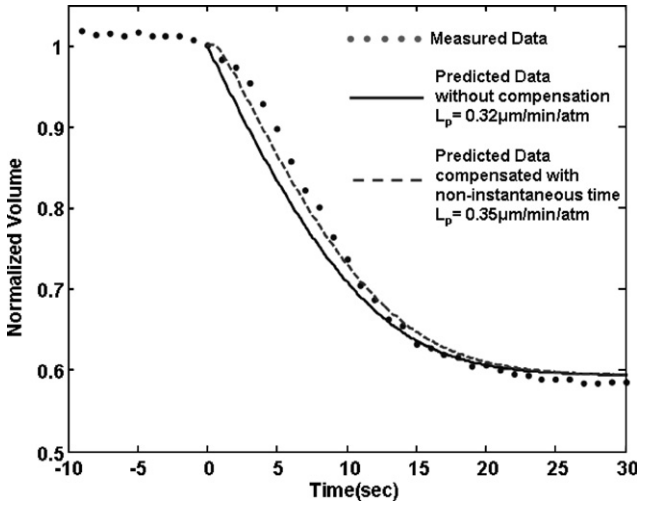

Fig. 11. Volume change of RBL cells in response to 3× PBS. Compensated curve-fitted line (dashed) according to Eqs. (1), (2), and (6) show 0.03 μm/min/atm (or 8%) increase of L_p compared with non-compensated curve-fitted line (solid).

We conclude that this device enables us to: (1) readily monitor the changes of extracellular conditions by rapidly perfusing a single cell or a group of cells with prepared media; (2) confine cells (or a cell) within a monolayer chamber, which prevents imaging ambiguity, such as cells overlapping or moving out of the focus plane; and (3) study cell osmotic response and determine cell membrane transport properties. In addition, this system is: (4) in-expensive and disposable for multiple usages and (5) allowed customizing the needed size and geometry of the chamber with just a change of the mask.

Acknowledgments

The authors thank Dr. Chihchen Chen and Dr. Chiahsien Hsu in the Folch Lab for providing RBL cells and for the help in fluorescent microscopic photographing, respectively. This work was supported by a grant from NIH FHCRC/UW Center for Medical Countermeasures against Radiation and a Gift grant from Washington Research Foundation.

References

[1] R.W. Applegate, J. Squier, T. Vestad, J. Oakey, D.W.M. Marr, Optical trapping, manipulation, and sorting of cells and colloids in microfluidic systems with diode laser bars, Optics Express 12 (2004) 4390–4398.
[2] F.G. Arnaud, D.E. Pegg, Permeation of glycerol and propane-1,2-diol into human platelets, Cryobiology 27 (1990) 107–118.
[3] D.A. Ateya, F. Sachs, P.A. Gottlieb, S. Besch, S.Z. Hua, Volume cytometry: microfluidic sensor for high-throughput screening in real time, Anal. Chem. 77 (2005) 1290–1294.
[4] P.G. Chao, A.C. West, C.T. Hung, Chondrocyte intracellular calcium, cytoskeletal organization, and gene expression responses to dynamic osmotic loading, Am. J. Physiol. Cell Physiol. 291 (2006) 718–725.
[5] J.K. Critser, A.R. Huse-Benda, D.B. Aaker, B.W. Arneson, G.D. Ball, Cryopreservation of human spermatozoa. I. Effects of holding procedure and seeding on motility, fertilizability and acrosome reaction, Fertil. Steril. 50 (1988) 314–320.
[6] H. Davson, J.F. Danielli, The Permeability of Natural Membranes, second ed., Cambridge University Press, Cambridge UK, 1952.
[7] D.C. Duffy, J.C. McDonald, O.J.A. Schueller, G.M. Whitesides, Rapid prototyping of microfluidic systems in poly(dimethylsiloxane), Anal. Chem. 70 (1998) 4974–4984.
[8] D.Y. Gao, C.T. Benson, C. Liu, J.J. McGrath, E.S. Critser, J.K. Critser, Development of a novel microperfusion chamber for determination of cell membrane transport properties, Biophys. J. 71 (1996) 443–450.
[9] D.Y. Gao, J. Liu, C. Liu, L.E. McGann, P.F. Watson, F.W. Kleinhaus, P. Mazur, E.S. Critser, J.K. Critser, Prevention of osmotic injury to human spermatozoa during addition and removal of glycerol, Hum. Reprod. 10 (1995) 1109–1122.

[10] D.Y. Gao, J.J. McGrath, J. Tao, C. Benson, E.S. Critser, J.K. Critser, Membrane transport properties of mammalian oocytes: a micropipette perfusion technique, J. Reprod. Fertil. 102 (1994) 385–392.
[11] J.A. Gilmore, L.E. McGann, J. Liu, D.Y. Gao, A.T. Peter, F.W. Kleinhans, J.K. Critser, Effect of cryoprotectant solutes on water permeability of human spermatozoa, Biol. Reprod. 53 (1995) 985–995.
[12] J.B. Heymann, P. Agre, A. Engel, Progress on the structure and function of aquaporin 1, J. Struct. Biol. 121 (1998) 191–206.
[13] D. Huh, W. Gu, Y. Kamotani, J.B. Grotberg, S. Takayama, Topical review: microfluidics for flow cytometric analysis of cells and particles, Physiol. Meas. 26 (2005) R73–R98.
[14] J.E. Hunter, B.J. Fuller, J.J. McGrath, R.W. Shaw, Measurements of the membrane water permeability (L_p) and its temperature dependence (activation energy) in human fresh and failed-to-fertilize oocytes and mouse oocyte, Cryobiology 29 (1992) 240–249.
[15] M.H. Jacobs, The simultaneous measurement of cell permeability to water and to dissolved substances, J. Cell. Comp. Physiol. 2 (1932–1933) 427–444.
[16] F.W. Kleinhans, V.S. Travis, J. Du, P.M. Villines, K.E. Colvin, J.K. Critser, Measurement of human sperm intracellular water volume by electron spin resonance, J. Androl. 13 (1992) 498–506.
[17] F.W. Kleinhans, Membrane permeability modeling: Kedem-Kathalsky vs a two-parameter formalism, Cryobiology 37 (1998) 271–289.
[18] S.P. Leibo, Water permeability and its activation energy of fertilized and unfertilized mouse ova, J. Membr. Biol. 53 (1980) 179–188.
[19] C. Liu, C.T. Benson, D.Y. Gao, B.W. Haag, L.E. McGann, J.K. Critser, Water permeability and its activation energy for individual hamster pancreatic islet cells, Cryobiology 32 (1995) 493–502.
[20] B. Lucke, M. McCutcheon, The living cell as an osmotic system and its permeability to water, Physiol. Rev. 12 (1932) 68–138.
[21] R.I. Macey, R.E.L. Farmer, Inhibition of water and solute permeability in human red cells, Biochim. Biophys. Acta 211 (1970) 104–106.
[22] P. Mazur, The role of intracellular freezing in the death of cells cooled at supraoptimal rates, Cryobiology 14 (1977) 251–272.
[23] P. Mazur, Equilibrium, quasi-equilibrium and nonequilibrium freezing of mammalian embryos, Cell Biophys. 19 (1990) 53–92.
[24] P. Mazur, Is intracellular ice formation the cause of death of mouse sperm frozen at high cooling rates? Biol. Reprod. 66 (2002) 1485–1490.
[25] J.C. McDonald, D.C. Duffy, J.R. Anderson, D.T. Chiu, H. Wu, O.J.A. Schueller, G.M. Whitesides, Fabrication of microfluidic systems in poly(dimethylsiloxane), Electrophoresis 21 (2000) 27–40.
[26] L.E. McGann, A.R. Turner, J.M. Turc, Microcomputer interface for rapid measurement of average volume using and electronic particle counter, Med. Biol. Eng. Comput. 20 (1982) 117–120.
[27] L.E. McGann, M. Stevenson, K. Muldrew, N. Schachar, Kinetics of osmotic water movement in chondrocytes isolated from articular cartilage and application to cryoperservation, J. Orthop. Res. 6 (1988) 109–115.
[28] L.E. McGann, H.Y. Yang, M. Walterson, Manifestations of cell damage after freezing and thawing, Cryobiology 25 (1988) 178–185.
[29] J.J. McGrath, A Microscope diffusion chamber for the determination of the equilibrium and non-equilibrium osmotic response of individual cells, J. Microsc.-Oxford 139 (1985) 249–263.
[30] J.J. McGrath, Quantitative measurement of cell membrane transport: technology and application, Cryobiology 34 (1997) 315–334.
[31] K. Muldrew, L.E. McGann, The osmotic rupture hypothesis of intracellular freezing injury, Biophys. J. 66 (1994) 532–541.
[32] M.K. Ng Jessamine, I. Gitlin, A.D. Stroock, G.M. Whitesides, Components for integrated poly(dimethylsiloxane) microfluidic systems, Electrophoresis 23 (2002) 3461–3473.
[33] C.V. Paganelli, A.K. Solomon, The rate of exchange of tritiated water across the human red cell membrane, J. Gen. Physiol. 41 (1957) 259–270.
[34] F. Penninckx, S. Poelmans, R. Kerremans, W. De Loecker, Erythrocyte swelling after rapid dilution of cryoprotectants and its prevention, Cryobiology 21 (1984) 25–32.
[35] D. Qin, Y. Xia, G.M. Whitesides, A rapid prototyping method for generating patterns and structures with feature sizes larger than 20 μm, Adv. Mater. 8 (1996) 917–919.
[36] M. Toner, E.G. Cravalho, M. Karel, Thermodynamics and kinetics of intracellular ice formation during freezing of biological cells, J. Appl. Phys. 69 (1990) 1582–1593.
[37] H. Takamatsu, Y. Komori, S. Zawlodzka, M. Fujii, Quantitative examination of a perfusion microscope for the study of osmotic response of cells, J. Biomech. Eng. 126 (2004) 402–409.
[38] A. Tourovskaia, X. Fiqueroa-Masot, A. Folch, Differentiation-on-a-chip: a microfluidic platform for long-term cell culture studies, Lab Chip 5 (2005) 14–19.
[39] G.M. Whitesides, E. Ostuni, S. Takayama, X. Jiang, D.E. Ingber, Soft lithography in biology and biochemistry, Annu. Rev. Biomed. Eng. 3 (2001) 335–373.
[40] Y. Xia, G.M. Whitesides, Soft lithography, Annu. Rev. Mater. Sci. 28 (1998) 153–184.